Pathways and their usage in the conversion of carbohydrates by aqueous barium hydroxide

insights from hyperpolarized and quantitative NMR

Hansen, Allan R.E.; Jensen, Pernille R.; Meier, Sebastian

Published in:
Catalysis Science & Technology

Link to article, DOI:
https://doi.org/10.1039/D2CY01519F

Publication date:
2023

Document Version
Peer reviewed version

ARTICLE

Pathways and their usage in the conversion of carbohydrates by aqueous barium hydroxide: insights from hyperpolarized and quantitative NMR

Received 00th January 20xx,
Accepted 00th January 20xx

DOI: 10.1039/x0xx00000x

Allan R.E. Hansen,[a] Pernille R. Jensen,[b] and Sebastian Meier[a]*

The conversion of lignocellulosic biomass and its components (carbohydartes, lignin) to precursor chemcials is expected to both expand the range of industrial chemicals and to reduce the dependence on fossil resoucres. Challenges in the green transition arise from the multifunctionality of biosourced reactants and from the difficulty in identifying highly selective processes for their conversion to useful precursors. Among the promising precursor molecules that can be derived from carbohydrates through chemocatalysis are lactate and its ester variants. Chemocatalytic conversion of glucose by concentrated aqueous solutions of barium hydroxide at ambient temperatures in the absence of oxygen has been described as highly selective, but high-resolution NMR or MS characterizations of the product mixture and mechanistic insights are sparse. Here, we employ sensitivity enhanced ("hyperpolarized") NMR to track the reaction cascade of hexose conversion by barium hydroxide and directy visualize transient enol and dihydroxyacetone species as the intermeditaes in the chemocatalytic pathway, similar to biochemical glycolysis. Quantitative NMR indicates that the conversion of glucose by barium hydroxide under anaerobic conditions indeed is highly selective for the formation 2-hydroxy-3-deoxy acids, which can include longer equivalents than lactate. C4-C6 analogues (metasaccharinic acids) can in total account for nearly the same carbon fraction as lactate in a reaction avoiding the formation of oxidation products.

Introduction

The conversion of bio-sourced molecules to fuels and chemicals is a central challenge in the green transition. Bio-sourced substrates are rapidly replenished in nature and afford a sustainable use of carbon without burdening the atmosphere with greenhouse gases and without exhausting fossil resources that are non-uniformly distributed on earth. Among the bio-sourced substrates, the C6 sugars glucose and its ketose isomer fructose have outstanding importance as prime products formed in photosynthesis and as components of structural and storage saccharides. Hence, these abundant C6 sugars (hexoses) are available at attractive costs in pure form.

The conversion of C6 sugars to value-added chemicals and fuels at high selectivity and low cost is unfortunately not trivial. A central obstacle to selective low-cost reactions is the polyfunctional nature of carbohydrates, encompassing several hydroxy groups. This polyfunctionality often leads to several isomeric substrate, intermediate and product forms, whose separation can be costly, labour-intensive and often also impossible.[1] Consequently, achieving high selectivity in the conversion of glucose remains a prime objective in the green transition. The design of suitable processes requires insight into the catalytic pathways of carbohydrate conversion. Such insights can remain challenging, as isomeric forms of carbohydrates and their dehydration or cleavage products need to be distinguished. Fortunately, ever-improving methodologies for guiding biomass conversion are being developed and encompass for instance NMR spectroscopy,[2–10] optical operando spectroscopy,[11–13] X-ray diffraction or absorption spectroscopy,[14] inelastic neutron scattering,[15,16] and DFT calculations.[17–20]

Among the chemicals that can be derived from hexoses are lactic acid (2-hydoxypropanoic acid) and its esters. Lactic acid and its esters are mostly relevant as building blocks of biodegradable plastics,[21,22] but in addition they play a role in the food, pharmaceutical and chemical industries.[23] Most of the world production of lactic acid derives from fermentation, but long fermentation times, costly media and low productivity have been described as obstacles in the biotechnological production.[23] Hence, chemocatalytic approaches for the production of lactate or its esters remain interesting. A wide variety of selectivities has been reported when converting glucose with Lewis acidic or Brønsted basic homogeneous or heterogeneous catalysts.[20–29] Especially the use of barium

[a] Department of Chemistry, Technical University of Denmark, Kemitorvet, Bulding 207, 2800 Kgs Lyngby, Denmark
[b] Department of Health Technology, Technical University of Denmark, Elektrovej 349, 2800 Kgs Lyngby, Denmark
† Footnotes relating to the title and/or authors should appear here.
Electronic Supplementary Information (ESI) available: [details of any supplementary information available should be included here]. See DOI: 10.1039/x0xx00000x

hydroxide ($Ba(OH)_2$) under anaerobic conditions has been described to give almost quantitative conversion of glucose at room temperature according to HPLC analyses.[23] The current study set out to probe the reaction pathways of barium hydroxide mediated glucose conversion with state of the art reaction tracking and quantitative NMR (qNMR). We visualize transient enol and dihydroxyacetone species as intermediates in the chemocatalytic pathway, somewhat analogous to biochemical glycolysis. Quantitative NMR shows that the conversion of glucose by barium hydroxide under anaerobic conditions indeed is highly selective for the formation of a homologous series of 2-hydroxy-3-deoxy acids. However, C4-C6 variants (metasaccharinic acids) can contribute to a similar degree to the carbon balance as lactate itself does.

Results and discussion

D-DNP indicates the formation of enol, 1,2 dicarbonyl compounds and dihydroxyacetone as central intermediates

Glucose is both the principal product of photosynthesis and the substrate of glycolysis. The biological conversion of glucose proceeds through a retro-aldol reaction upon isomerization to (phosphorylated) fructose and cleavage into C3 sugars, or alternatively by the Entner-Doudoroff pathway proceeding through a 3-deoxy intermediate that is formed following a dehydration step. The flux of C6 substrates through glycolysis is often difficult to follow, but has been visualized recently through ^{13}C NMR methods employing D-DNP.[30,31] In these methods, nuclear magnetization of ^{13}C in a probe molecule is temporarily redistributed in a dedicated instrument, affording NMR sensitivity gains (hyperpolarization) of several orders of magnitude for fast reactions on the seconds timescale.[32] When employing C6 sugars as substrates, the method depends on the use of isotopologues with non-protonated sites, as signal enhancement is lost with the T_1 time, which is shorter for protonated than for non-protonated sites.

We initially investigated the conversion of [U-^{2}H,^{13}C] glucose and of [2-^{13}C] fructose by barium hydroxide using D-DNP NMR. Even at elevated temperatures (near 60 °C), glucose conversion by 0.25 M $Ba(OH)_2$ to lactate on the seconds time scale was limited (Fig. S1). In addition to some lactate signal, a faster appearance of a signal near 40.5 ppm was detected. Among the plausible products of glucose,[33,34] this CH_2 chemical shift is characteristic for the 3-deoxy compound 3-deoxyglucosone, an intermediate that had previously been described as a plausible intermediate in the conversion of carbohydrates by metal hydroxides.[35] The formation of 3-deoxyglucosone from glucose entails the loss of water, similar to the mechanisms in the initial stages of the Entner-Doudoroff pathway.

Opposite to the conversion of [U-^{2}H,^{13}C] glucose by barium hydroxide, the conversion of [2-^{13}C] fructose proceeded significantly faster under else identical conditions (Fig. 1), leading to larger product signal on the seconds timescale. In the conversion of glucose, fructose is a likely intermediate prior to the formation of two C3 sugar intermediates and their isomerization to lactate. The D-DNP experiments of Figure 1 highlight that glucose is formed from fructose, thus highlighting that a pre-equilibrium between glucose and fructose channels fructose towards retro-aldol cleavage of fructose to two C3 sugars. Notably, the anomeric forms of fructose were in intermediate exchange indicative of millisecond dynamics in the presence of 0.25 M $Ba(OH)_2$ at 60°C, while the acyclic form of fructose was not detected even with 10000-fold ^{13}C NMR enhancement through D-DNP, indicative of rapid cyclization and/or cleavage of the open chain form. In the conversion of hyperpolarized [2-^{13}C] fructose, the formation of enol signals near 149 and 154 ppm in the ^{13}C NMR spectrum becomes apparent. Enol species (including enediolates, Fig. 1 bottom) are plausible intermediates in the barium hydroxide catalysed conversion of hexoses, but their presence is difficult to directly show in the absence of hyperpolarization, unless enol species are stabilized by Lewis acidic metal ions.[3] The detection of enol species at C2 indicates that the presence of oxygen in this site affords coordination to barium hydroxide.

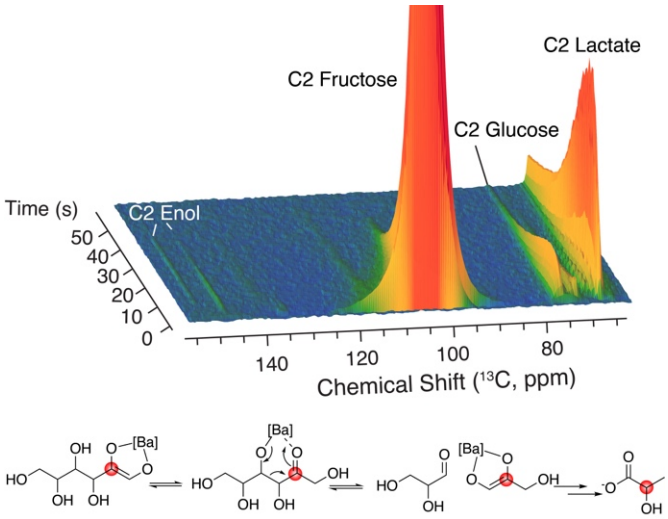

Fig. 1 D-DNP experiment showing the conversion of hyperpolarized [2-^{13}C] fructose in the presence of barium hydroxide. A time series of ^{13}C NMR spectra was acquired using a 10° flip angle pulse. Signals from the C2 position of glucose and lactate emerge alongside enol species within one minute. Overall, signal fades due to the loss of hyperpolarization with T_1. Reaction conditions: 250 mM $Ba(OH)_2$, 6 mM hyperpolarized [2-^{13}C] fructose, 60 °C, D_2O solvent.

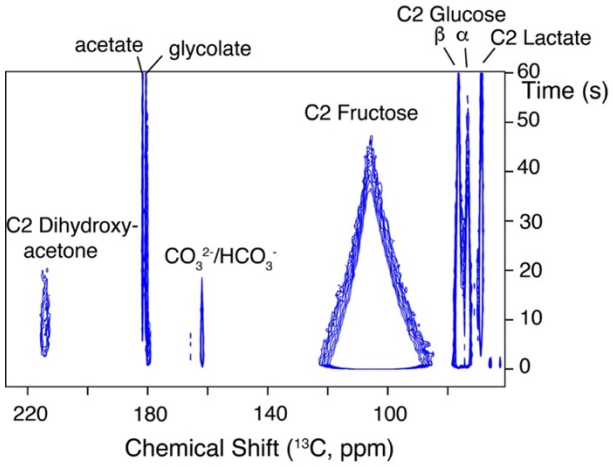

Fig.2. D-DNP experiment showing the conversion of hyperpolarized [2-^{13}C] fructose in the presence of a lower concentration barium hydroxide than in Fig.1. A top-down view on a series of 1D ^{13}C NMR spectra acquired using a 10° flip angle pulse is shown. Reaction conditions: 50 mM $Ba(OH)_2$, 6 mM hyperpolarized [2-^{13}C] fructose, 60 °C, D_2O solvent.

Both the slow entry of substrate via glucose and the rapid conversion of fructose to lactate and glucose in the presence of 0.25 M barium hydroxide made it difficult to directly detect other intermediates. Hence, the D-DNP observation of fructose conversion was repeated in the presence of lower amounts of barium hydroxide (0.05 M). In this experiment, the formation of a free keto group deriving from the fructose C2 position was evident from a ^{13}C NMR signal near 214.1 ppm. The emergence of this signals was indicative of the expected formation of dihydroxyacetone in a retro-aldol step from fructose. Overall, the D-DNP experiments thus indicate that glucose and fructose interconvert through aldose-to-ketose isomerization, while fructose ring forms and the open chain form equilibrate rapidly. Fructose reacts rapidly to lactate in a pathway, for which C2-enol and dihydroxyacetone intermediates are directly detectable. The conversion of glucose through fructose, dihydroxyacetone and C2-enol species remarkably resembles conventional Embden-Meyerhof-Parnas glycolysis, which converts glucose to fructose-phosphates, C3-sugar phosphates including dihydroxyacetone phosphate, and organic C3 acids in most organisms. In contrast, the competing influx of glucose carbons into a pathway that entails the formation of 3-deoxyglucosone bears similarity to the upper part of Entner-Doudoroff glycolysis, which is an alternative glycolytic pathway in some bacteria and possibly plants that converts glucose via a key 3-deoxyacid intermediate.

The D-DNP experiment of Figure 2 was conducted in an NMR tube without attempts to exclude air oxygen, to concurrently probe influx into competing pathways for the oxidative degradation of glucose and fructose. Indeed, the conversion of C_2 to the carboxyl group of acetate and glycolate could be observed alongside the formation of carbonate, formate and longer degradation products. These observations indicate that byproducts in the barium hydroxide reaction system derive from the oxidative cleavage of adjacent carbonyls (α-dicarbonyl cleavage)[35] in the presence of air oxygen. The plausible reaction pathways of Scheme 1 underline that dicarbonyl compounds including, but not limited to, 3-deoxyglucosone can be formed in aqueous hexose/barium hydroxide mixtures. In contrast, other previously reported by-products attributed to the presence of oxygen such as glyceraldehyde, malonic acid and glyceric acid[23] were not observed with NMR spectroscopy to any significant amounts.

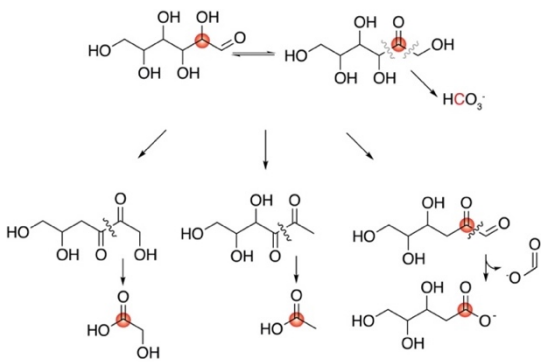

Scheme 1. Plausible reaction pathways to byproducts such as glycolate, acetate and formate in aqueous hexose/barium hydroxide mixtures.

NMR mixture analysis on post-reaction material after anaerobic conversion

Subsequently, we employed high-resolution NMR spectroscopy to track the conversion of carbohydrates in aqueous barium hydroxide (0.25 M) solution on a slower time scale. Fig. 3 displays the time series of glucose conversion as followed with a series of ^1H NMR spectra. Surprisingly, various species containing an aliphatic CH_2 group emerged as stable products in parallel to lactate. None of the previously described byproducts of the reaction (formate, malonate, glycolate, glycerate, glyceraldehyde) contain an aliphatic CH_2 group, while D-DNP experiments had indicated the possibility that 3-deoxyspecies such as 3-deoxyglucosone can be formed.

After the reaction of Figure was completed, homonuclear and heteronuclear 2D NMR assignment spectra were acquired to identify the molecular species containing aliphatic CH_2 groups. Structural determinations and corresponding chemical shift assignments of molecules in the reaction mixture are displayed in Fig. 4. Notably, these species were subsequently also identified in anaerobic reaction mixtures. Byproducts include a series of homologous 2-hydroxy-3-deoxy acids representing C4-C6 analogues of lactic acid (entries **2**, **4**, and **5** in Fig.4; Fig. S2, ESI†). Beyond multidimensional assignment spectra, ^1H diffusion ordered spectroscopy (Fig. S3, ESI†) was used to validate the presence

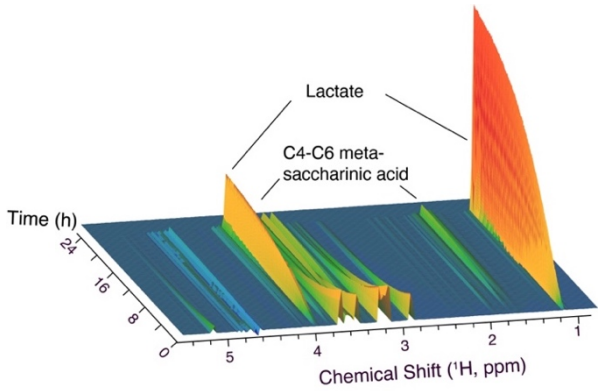

Fig. 3 Time series of conventional ^1H NMR acquired on an 800 MHz instrument equipped with a TCI cryoprobe with a time resolution between individual ^1H NMR spectra of 3.1 minutes. Reaction conditions: 250 mM Ba(OH)2, 100 mM glucose, 30 °C, 90% H_2O/10% D_2O (500 µl).

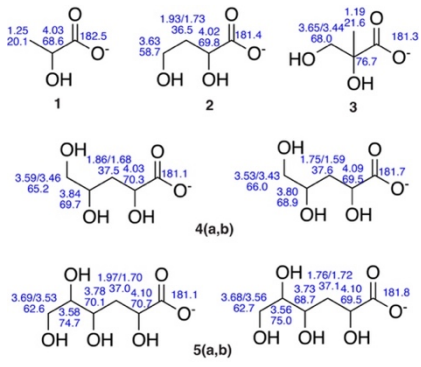

Fig. 4 Chemical shift assignments of molecules identified in the glucose conversion by barium hydroxide, both in the presence and in the absence of air oxygen.

alcohol and methylene group signals with slower translational diffusion than lactate in molecules **2**, **4**, and **5**. The formation of metasaccharinic acids indicates that reactions proceeding from C3 carbohydrates to lactate are paralleled by similar reactions for C4, C5 and C6 carbohydrates. These compounds form one NMR spectral species for C4, while the C5 and C6 variants occur in two diastereomeric forms. The occurrence of only one C4 form can be attribute to the presence of one single stereogenic centre at C2. Different stereoisomers at C2 will hence be enantiomers in the C4 metasaccharinic acid and will not be distinguishable by NMR spectroscopy. In contrast, the C5 and C6 metasaccharinic acid occur as pairs of diastereomers. Isomerization at the C2 position is consistent with the formation of metasaccharinic acids through intermediates with sp^2 hybridized C2 such as enol and 1,2 dicarbonyl species.

In addition to the C4-C6 metasaccharinic acids **2**, **4**, and **5**, a branched C4 saccharinic acid **3** (Fig. 4) containing a quaternary carbon was identified. The formation of this compound can be plausibly explained through a benzylic acid rearrangement as shown in Scheme 2. The likely substrate for this product is a 2,3 dicarbonyl compound, akin to the plausible substrate for the formation of glycolate (see Scheme 1) in the presence of air oxygen. Notably, all the products of Fig. 4 that formed in the absence of oxidant indeed form by overall redox neutral conversions.

Quantitative NMR spectroscopy (qNMR) was subsequently used to probe the carbon balance in the reaction mixture under anaerobic conditions. NMR spectroscopy is a quantitative method, if care is taken to ensure that all detected nuclear spins have the same polarization (i.e., alignment of nuclear magnetic moments with the magnetic field) prior to the measurement. This condition is met by waiting sufficiently long between acquisitions to ensure equilibrium polarization for all detected molecular sites or through calibration of response factors[36] for the used experiments relative to quantitative experiments. Required waiting times in quantitative experiments were shortened through the addition of paramagnetic additives to improve sensitivity and shorten time demand.[2,37,38] Careful qNMR quantifications of the detected species after varying reaction times and temperatures are shown in Fig. 5 (and Fig. S4-S7, ESI†). These data show an unsurprising acceleration of glucose conversion with increasing reaction temperatures. Glucose conversion according to these samples withdrawn from an ongoing reaction were quenched by the addition of sulfuric acid. Glucose conversion both of the *in situ* NMR experiment of

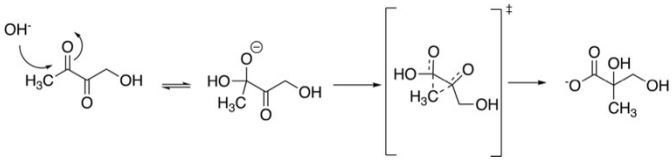

Scheme 2. Plausible mechanism for the formation of a C4 saccharinic acid identified in the reaction mixture for glucose conversion by barium hydroxide.

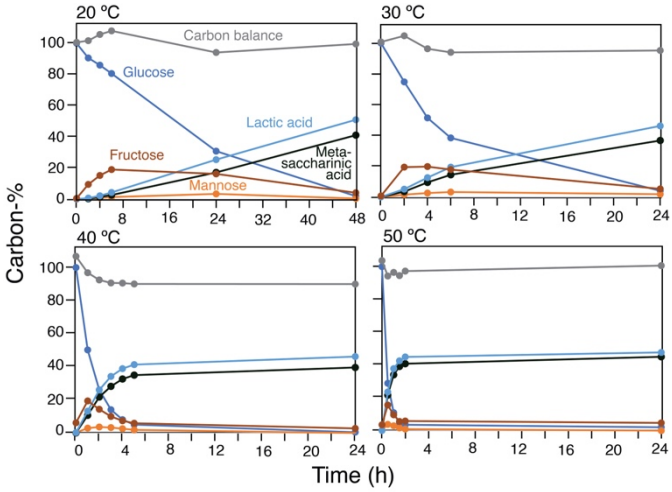

Fig. 5 Quantification of carbon-percentage in major reactants, intermediates, and products in the conversion of glucose with barium hydroxide at varying temperatures. The carbon balance is given from the sum of carbon atoms in different molecular species. Reaction conditions: 250 mM $Ba(OH)_2$, 100 mM glucose, variable temperature and time as indicated, nitrogen atmosphere, H_2O solvent.

Fig. 3 (see Fig. S8, ESI† for integrals) and of the time-discrete analyses of Fig. 5 were well described by an exponential decay and hence first order kinetics. The temperature dependence of reaction rate constants derived from the data of Fig. 5 was subjected to Arrhenius analysis, yielding an energy of activation of 102 ± 5 kJ/mol (Fig. S9, ESI†).

Quantifications of fructose, mannose (Fig. S10 and S11, ESI†), metasaccharinic acids, and lactate were conducted alongside the identification and quantification of formate and acetate. Using qNMR and accounting for metasaccharinic acids, a carbon balance above 90% was found for all temperatures and all time points for anaerobic samples. Dihydroxyacetone could be detected at a low steady state concentration in the reaction mixtures when employing [1-^{13}C] glucose as the substrate and using HSQC detection (Fig. S12, ESI†), while the previously reported aldose isomer glyceraldehyde was not detected,[23] consistent with the higher expected stability and equilibrium concentration of the acyclic ketose relative to the aldose form. The observed formation of mannose was consistent with the formation of glucose, fructose, and mannose from a common enediol intermediate. Fructose was found to accumulate to levels near 20% at all temperatures, consistent with values previously reported for the reaction system.[23]

Even though their ^{1}H NMR signals are not prominent, the sum of metasaccharinic acid species contained similar amounts of carbon as lactate in the anaerobic conversions of glucose detected herein. Such species have previously not been included in HPLC quantifications, possibly due to the lack of commercially available reference compounds. This example showcases the benefit of detecting and identifying novel molecular species in the absence of authentic standards through NMR. The low signal intensity of the metasaccharinic acids in ^{1}H NMR is the compounded effect of several factors: (i) metasaccharinic acids are longer than lactate with only two

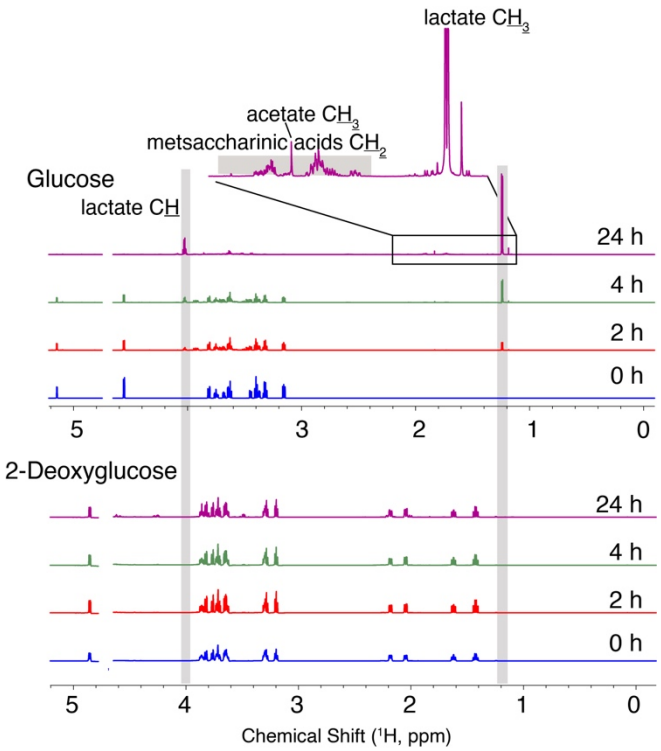

Fig. 6 Comparison of 1H NMR spectra obtained in the conversion of glucose (top, four time points) and of 2-deoxy glucose (bottom, identical time points as for glucose). The complex multiplets of chemically non-equivalent methylene protons in metsaccharinic acids are shown in the inset shown on top. Reaction conditions: 250 mM $Ba(OH)_2$, 100 mM hexose, 30 °C, nitrogen atmosphere, H_2O solvent.

hydrogens in a methylene group as compared to the methyl group of lactate, (ii) the hydrogens in the CH_2 group are non-equivalent due to the presence of stereogenic centres in the metasaccharinic acids and (iii) the individual hydrogen signals are split into broad multiplets (Fig. 6, top). This example demonstrates that significant carbon balance can be overlooked from compounds for which authentic standards are not easily accessible with chromatographic methods, while NMR detection may be hampered by the loss of signal intensity through the splitting of NMR signals by scalar coupling and chemical non-equivalence.

Mechanistic insight from various substrates and conditions

The conversion of glucose was repeated under identical conditions using a 2-deoxyglucose substrate. Opposite to the avid conversion of glucose itself, 2-deoxyglucose proved stable in our reaction setup (Figure 6). This finding indicates that C2 position is central to the anaerobic pathways of glucose conversion, consistent with the central role of 3-deoxyglucosone, 2-enols and fructose as reaction intermediates in the conversion of glucose. Hence, the selectivity and reactivity of barium hydroxide in retro-aldol cleavage and intramolecular dehydration and rehydration reactions seems to fully hinge on mechanisms including the C2 oxygen. This observation is further consistent with the intermediates of Scheme 1 that can be

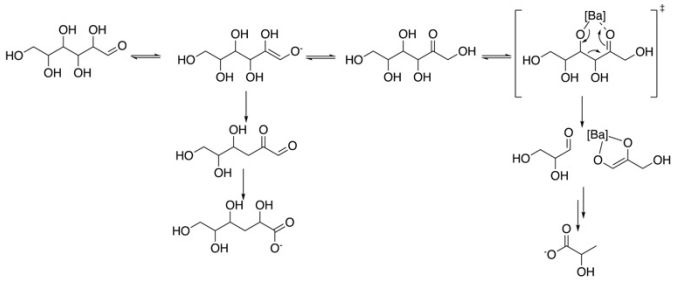

Scheme 3. Plausible mechanism for the formation of lactate and metasaccharinic acids (here C6) from glucose.

inferred from oxidative cleavage reactions under aerobic reaction conditions and that all maintain an oxygenated C2.

A plausible reaction pathway towards lactate and metasaccharinic acids based on the experimental observations from D-DNP NMR and conventional NMR is shown in Scheme 3. Glucose interconverts with fructose and can alternatively form 3-deoxyglucosone. Fructose is the plausible substrate for a 3+3 retro-aldol cleavage, while 3-deoxyglucose could be considered the C6 equivalent of methyl glyoxal that is rapidly converted to the corresponding 2-hydroxy-3-deoxy acid. In addition to the C6 metasaccharinic acid, glucose primarily forms the racemic C4 metasaccharinic acid. This observation is consistent with a 4+2 retro-aldol cleavage of glucose prior to the conversion of the C4 sugar in analogy to the conversion of C3 sugar to lactate. The fraction of the metasaccharinic acids relative to lactate (Fig. 5) and their distributions in length were not systematically affected by the reaction temperature between 20 and 50 °C. In contrast, the length of the substrate had a stronger effect, where the fraction of carbon in metasaccharinic acids rather than lactate increased with decreasing chain length of the substrate (Fig. S14, ESI†).

Isotope studies were finally employed to gain additional mechanistic insight into the barium hydroxide catalysed glucose conversion. [1-^{13}C] glucose was employed as the substrate and the isotope distribution in the resultant lactate population was assessed. The majority of the C1 position (56%) was found in the methyl position of lactate, while 38% were found in the C1 position and 6% were found in the C2 position. This distribution is similar to distributions reported previously for the

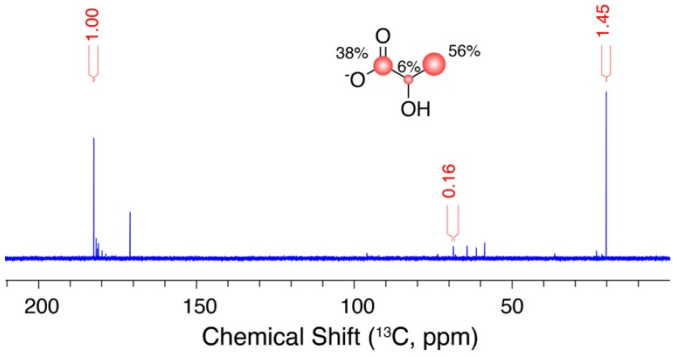

Fig. 7 Quantitative 1D ^{13}C NMR spectrum acquired to probe the isotope distribution in lactate following the conversion of [1-^{13}C] glucose. Reaction conditions: 250 mM $Ba(OH)_2$, 20 mM [1-^{13}C] glucose, 30 °C, nitrogen atmosphere, H_2O solvent, 24 hours reaction time.

conversion of [1-^{13}C] glucose by potassium hydroxide under anaerobic conditions.[35] The conversion of glucose to a free pool of symmetric dihydroxyacetone would give reason to believe that the isotope distribution in lactate should be equal at the C1 and C3 position. The slight asymmetry could be rationalised with a more concerted conversion entailing a rapid enolization in the C3 fragment prior to its conversion to lactate (Scheme 3). The presence of ^{13}C label at the C2 position beyond its natural abundance validates that C-C bond breakage and formation occurs beyond the retro-aldol 3+3 cleavage of fructose, leading to a scrambling of ^{13}C to the remaining position.

The reaction was conducted in D_2O to probe the incorporation of deuterium in different product classes. Unsurprisingly, the methyl group in lactate was predominantly singly (as expected for the C6 position in glucose) and doubly (as expected for C1, C3, and C4 positions in glucose) deuterated (Fig. 8).[39] The metasaccharinic acid species were predominantly deuterated at the methylene group (C3), consistent with their formation from 3-deoxyglucosone upon enolization of glucose. More surprisingly, not only the C3 position, but also the C4 position exhibited some deuterium incorporation, especially in C4 metasaccharinic acids, albeit deuteration at the methoxy group of C4 was lower than deuteration at methylene group of C3 (Fig. 8) in C4 metasaccharinic acids. Similarly, the saccharinic acid **3** formed through benzylic acid

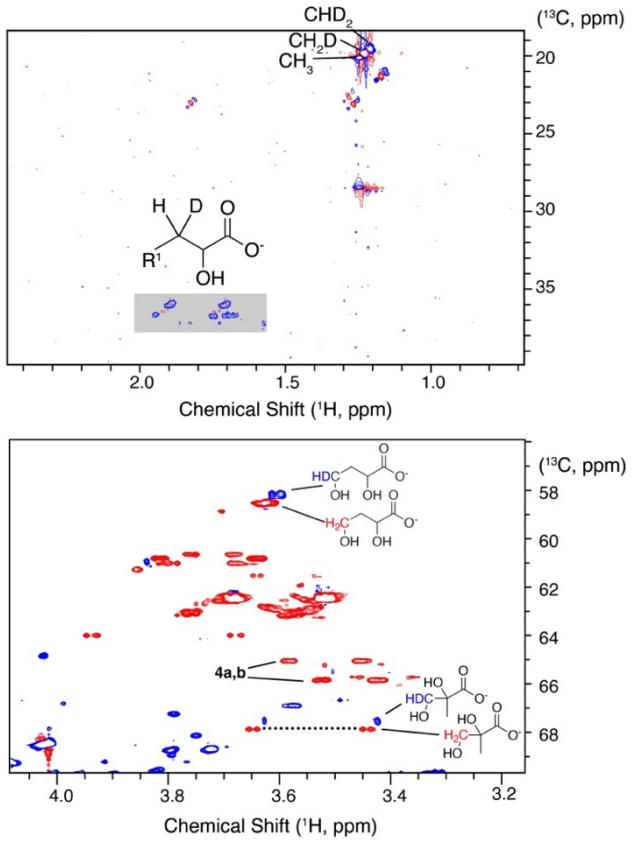

Fig. 8 Multiplicity-edited ^{1}H-^{13}C HSQC spectrum on a mixture obtained after reaction in D_2O. CH and methyl groups appear in blue while CH_2 groups appear in red. Spectral region of Reaction conditions: 250 mM $Ba(OH)_2$, 100 mM glucose, 30 °C, nitrogen atmosphere, D_2O solvent.

rearrangement (Scheme 2) exhibited deuteration in the methoxy group (Fig. 8, bottom). These observations overall indicate that barium can cause the loss of OH^- at C3 upon coordination to a C1-C2 enediolate and the loss of OH^- at C4 upon coordination to a C2-C3 enediolate (Scheme 4A). Such activity would also plausibly explain the efficient conversion of C3 carbohydrate intermediates into lactate according to the reaction sequence shown in Scheme 4B. Erythrulose was used as the substrate for barium hydroxide conversion to probe the reactions of Scheme 4A directly. Much higher conversion of erythrulose than of threose or other aldoses to the C4 saccharincic acid **3** was an indicator for the formation of 4-deoxyspecies through a reaction sequence similar to the one of Scheme 4A (Fig. S15 and S16, ESI†).

Various experimental results indicate an acyclic pathway towards 2-hydroxy,3-deoxy acids **1**, **2**, **4**, or **5**. Both the kinetic experiments showing a minor accumulation and high reactivity of acyclic dihydroxyacetone as compared to longer carbohydrate substrates, faster conversion of fructose than of glucose, and a larger influx of carbon into metasaccharinic acids **2**, **4**, or **5** (more efficient competition to the acyclic pathway from C3 carbohydrates) for the shorter carbohydrates among C4-C6 indicate a correlation between acyclic substrate fractions and reactivity (Fig. S17, ESI†). Such an acyclic conversion to the alpha-hydroxy acids has been considered unlikely for alkali hydroxides, due to stereoselective hydride transfer in 1,2 dicabonyl species.[35] Our results indicate that stereoselectivity in this step is low in aqueous alkaline barium hydroxide solutions, as evidenced by the equal distribution between the diastereomers **4a** and **4b** in Fig. 8. This equal distribution and low stereoselectivity in hydride transfer to C2 hence eliminates the central argument against an acyclic conversion pathway. Hence, the acyclic structures of Scheme 4A (top) seem the most plausible reactive species towards 2-hydroxy,3-deoxy acids for C4-C6 compounds.

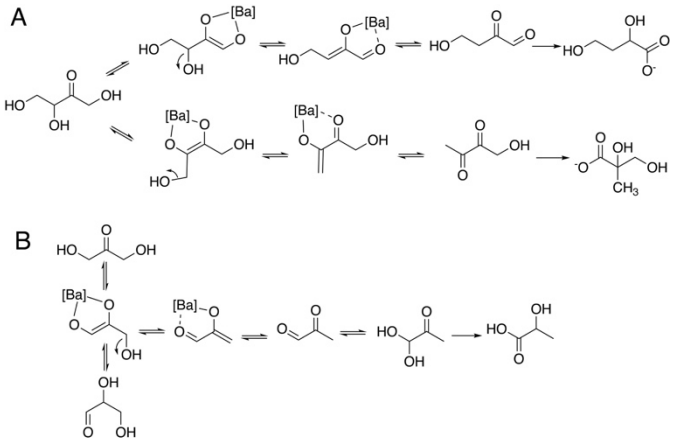

Scheme 4. Coordination of barium to enolate species involving oxygens on C1 and C2 or on C2 and C3 prior to elimination of adjacent hydroxy groups accounts for redox neutral products, for deuterium incorporation and for ^{13}C distributions. The emerging 1,2 dicarbonyl and 2,3 dicarbonyl species agree with those that also can be inferred from oxidative dicarbonyl cleavage.

Conclusions

In conclusion, we use NMR assays for an unbiased insight into the conversion of carbohydrates by aqueous barium hydroxide solutions. Direct observations using rapid-injection D-DNP NMR shows the formation of C2-enol species, dihydroxyacetone and 3-deoxyglucosone as intermediates. Notably, the C2-enol species were not detectable and hence likely lower populated in a control experiment following the conversion of glucose by aqueous sodium hydroxide (Fig. S18). To our surprise, we find high selectivity for a mixture of 3-deoxy carboxylic acids of length C3-C6 carrying hydroxyl groups on all other carbons. Isotope incorporation and product compositions under aerobic and anaerobic conditions indicate that C1-C2 and C2-C3 enediolates are formed. Upon retroaldol cleavage of fructose, dihydroxyacetone is detected as the principal intermediate *en route* to lactate. The retro-aldol cleavage of fructose to dihydroxyacetone as the principal intermediate that undergoes rapid conversion to lactate bears resemblance to the kinetic behaviour of the conventional Embden-Meyerhof-Parnas glycolysis. The formation of longer 3-deoxycarboxylic acids bears resemblance to the upper part of biochemical Entner-Doudoroff pathway.

Experimental

Materials. Chemicals including heavy water (D_2O, ≥99.9%), [1-^{13}C] glucose, [2-^{13}C] fructose and [U-^{13}C, U-^{2}H] glucose were all purchased from Sigma Aldrich (Andover, MA, USA) and used without further purification. Barium hydroxide was ordered as the octahydrate form (≥98%).

Dynamic Nuclear Polarization. Hyperpolarization of [2-^{13}C] fructose and of [U-^{13}C, U-^{2}H] glucose was conducted by dynamic nuclear polarization (DNP) and subsequent dissolution (D-DNP) as previously described:[31,40] briefly, solid state DNP was conducted using a mixture of trityl radical OX063 (4.6 mg; Oxford Instruments, Abingdon, UK), gadoteridol (3 mg of a 100 umol/g stock; Bracco Imaging, Italy), milliQ water (80.5 mg) and [2-^{13}C] fructose (106 mg) or [U-^{2}H,^{13}C] glucose (112 mg).

Preparations (20 mg) were placed in a sample cup and the samples were flash-frozen in liquid helium. Polarization transfer from trityl radicals to ^{13}C nuclei was performed at 1.2 K, using microwave irradiation at 93.89 GHz with 100 mW in a magnetic field of 3.35 T. This approach yielded solid-state polarizations above 30% after one hour. Upon dissolution with heated D_2O (5 mL), hyperpolarized samples with a final substrate concentration of 12 mM hexose were obtained. Of these hyperpolarized samples, 0.15 mL were manually injected into 0.3 mL of a 0.25 M aqueous solution of barium hydroxide octahydrate equilibrated to 70 °C inside a 500 MHz Bruker spectrometer equipped with a 5 mm DCH CryoProbe and a 11.7 T UltraShield magnet. This procedure yielded a final concentration of 4.0 mM hyperpolarized glucose in the NMR tube. The temperature upon mixing was determined to be approximately 60 °C.

Reactions were followed by a series of ^{13}C NMR spectra acquired with excitation by a pulse of nominal angle 10° and using both proton and deuterium decoupling. The spectra were acquired as pseudo-2D spectra using a receiver gain of 10 by sampling ^{13}C NMR FIDs of 24096 complex data points for 737 ms every second. The acquisition of NMR data was started prior to substrate injection, thus minimising the experimental dead-time.

Reaction procedure.
The catalytic reaction was conducted in a round bottomed flask equipped with a stirring-bar magnet and immersed in a water bath on a magnetic stirrer with heater at the desired temperature. Flasks were equipped with a septum stopper prior to degassing with N_2 overpressure through a syringe needle for 20 min. $Ba(OH)_2$ and desired carbohydrate solutions were flushed with an N_2 atmosphere in separate round bottomed flasks prior to transferring the carbohydrate substrate to the barium hydroxide solution using a stainless steel cannula and N_2 overpressure. Directly after mixing the two solutions a sample of 600 µL was extracted with a syringe and used as the reference for the following samples. While samples were extracted after desired times, an N_2 atmosphere was maintained to prevent contamination. After every subsequent sample extraction, N_2 flushing was maintained for 5 min. Each sample extraction of 600 µL was quenched with 400 µL phosphate buffer acidified with H_2SO_4 and the $BaSO_4$ was removed by centrifugation prior to freezing the samples until analysis. This procedure led to less than 0.5 carbon-% acetate and formate in the product mixture after full conversion of glucose, thus indicating that oxygen had been successfully excluded.

***Ex situ* NMR for assignments and quantification.**
A suite of homonuclear and heteronuclear 2D NMR experiments was used to assign chemicals in reaction mixtures produced by the conversion of C4-C6 sugars using aqueous barium hydroxide. ^{1}H–^{1}H COSY and TOCSY spectra were acquired using excitation sculpting for solvent suppression. ^{1}H–^{1}H COSY spectra were acquired by sampling the FID for 92 ms (1024 complex data points) and 27 ms (300 complex data points) in the direct and indirect dimension respectively (cosydfesgpphpp pulse program). ^{1}H–^{1}H TOCSY spectra were acquired with a 10 kHz spin lock field that was applied for 80 ms by sampling the FID for 128 ms (1024 complex data points) and 32 ms (256 complex data points) in the direct and indirect dimension respectively (dipsi2esgpph pulse program). ^{1}H-^{13}C HSQC spectra with and without multiplicity editing were acquired as data matrices of 1024 (^{1}H) × 200 (^{13}C) complex data points sampling the FID for 80 ms and 9 ms, respectively. ^{1}H-^{13}C HSQC spectra with multiplicity editing (hsqcedetgpsisp2.3) were acquired as data matrices of 2048 (^{1}H) × 400 (^{13}C) complex data points sampling the FID for 183 ms and 22 ms, respectively, using non-uniform sampling of 20% of the data points in the indirect dimension. ^{1}H-^{13}C HSQC spectra without multiplicity editing (hsqcetgp) were acquired as data matrices of 1024 (^{1}H) × 200 (^{13}C) complex data points sampling the FID for 160 ms and

17 ms, respectively, while employing non-uniform sampling of 50% of the data points in the indirect dimension.

A DOSY spectrum was acquired using stimulated echo and longitudinal eddy current delay (ledbpgp2s pulse program) prior to sampling 8192 complex data points during an acquisition time of 1.7 s and employing a diffusion time of 60 ms and a diffusion gradient length of 1.0 ms. DOSY was processed in Topspin 4.1.3 and further validated the presence of metsaccharinic acids with methylene groups, alcohol groups, and a slower translational diffusion than lactate.

For quantification, one-dimensional ^{1}H NMR spectra were acquired on a Bruker Avance III 800 MHz instrument equipped with a TCI Cryoprobe and a SampleJet sample changer using presaturation and composite pulse (zgccppr pulse program) sampling 16384 complex data points in the FID for 1.28 s. The response in this experiment was calibrated by comparison between two samples, one of which contained 1 mM ProHance® as a relaxation agent to account for the lower signal area arising from slow T_1 relaxation for formate and acetate ^{1}H NMR signals. Quantifications of metasaccharinic acids were obtained by integrating C4, C5 and C6 species in a ^{1}H-^{13}C HSQC spectrum acquired at 800 MHz to calculate the average length of the metasaccharinic acids. The carbon fraction in metasaccharinic acids relative to lactate could then be derived from ^{1}H NMR integrals by considering the fraction of the metasaccharinic acid methylene signal relative to the lactate methyl signal (typically around 30% for glucose substrate) and taking the number of protons (two in the methylene and three in the methyl group) into account to get molar ratios (typically 45%). The molar ratios then could be converted to ratios in carbon content by considering the length of metasaccharinic acids (approximately 5 carbons on average) relative to the three carbon atoms of lactate, yielding typical fractions of carbon in metasaccharinic acids that are approximately 75% the carbon in lactate.

For the quantification of ^{13}C distributions in lactate, the reaction mixture derived from the conversion of 20 mM [1-^{13}C] glucose for 24 hours at 30 °C by 0.25 M $Ba(OH)_2$, was subjected to quantitative ^{13}C NMR. To this end, a ^{13}C NMR spectrum using a 30° excitation pulse and inverse gated decoupling was acquired on a Bruker Avance III 800 MHz instrument equipped with a TCI Cryoprobe and a SampleJet sample changer. The FID was sampled for 1.4 s with 65536 complex data points and an inter-scan relaxation delay of 300 seconds between 64 accumulations.

Real time kinetic NMR assays. The conversion of glucose by aqueous barium hydroxide was directly followed on an 800 MHz Bruker Avance III instrument equipped with a 5 mm TCI cryoprobe and an Oxford magnet. A time series of ^{13}C NMR spectra (30° flip angle and inverse gated decoupling of ^{1}H) was acquired by accumulating 160 transients with an interscan relaxation delay of 4 seconds and sampling the FID for 0.68 s (32768 complex data points). The time series of ^{13}C NMR spectra was implemented as pseudo-2D experiments. This experiment acquired 128 time points (individual ^{13}C NMR spectra) with a time resolution of 12.5 min (duration of each individual spectrum). A sample of [1-^{13}C] glucose was dissolved to 100 mM concentration in 0.25 M $Ba(OH)_2$ and the reaction was followed at 50 °C to yield the time course of Figure S10. Equivalently, natural abundance glucose was dissolved to 100 mM concentration in 0.25 M $Ba(OH)_2$ and the reaction was followed by a pseudo-2D spectrum comprised of 512 individual 1D ^{1}H NMR spectra acquired by sampling 16384 complex data points for 1.47 s with an inter-scan relaxation delay of 10 seconds to yield the time course of Fig. 3 and Fig. S8 at 30 °C. Experiments followed in the NMR tube proceeded noticeably slower than corresponding experiments acquired in the presence of stirring.

NMR data acquisition and analysis software. All conventional (non-DNP) NMR spectra were acquired using Topspin 3.5 and were processed with ample zero filling and analyzed in Bruker Topspin 4.1.3. D-DNP spectra were acquired using Topspin 4.1.4.

Data Fitting. Exponential fits of glucose conversion were conducted with pro Fit 7 (QuantumSoft). Linear fits of the natural logarithm of the rate constants were plotted against the inverse absolute temperature. The slope was used to determine the energy of activation (Fig. S9, ESI†).

Conflicts of interest

There are no conflicts to declare

Acknowledgements

The authors gratefully acknowledge support by the Danish National Research Foundation (DNRF124) and the Independent Research Fund, Denmark (Green Transition Programme, Grant 0217-00277A). 800 MHz NMR spectra were recorded at the NMR Center DTU, supported by the Villum Foundation.

Notes and references

1 L. Lin, X. Han, B. Han and S. Yang, *Chem. Soc. Rev.*, 2021, **50**, 11270–11292.
2 A. R. E. Hansen, K. Enemark-Rasmussen, F. A. A. Mulder, P. R. Jensen and S. Meier, *J. Phys. Chem. C*, 2022, **126**, 11026–11032.
3 P. R. Jensen and S. Meier, *Chem. Comm.*, 2020, **56**, 6245–6248.
4 S. Meier, M. Karlsson and P. R. Jensen, *ACS Sus. Chem. Eng.*, 2017, **5**, 5571–5577.
5 S. Heikkinen, M. M. Toikka, P. T. Karhunen and I. A. Kilpeläinen, *J. Am. Chem. Soc.*, 2003, **125**, 4362–4367.
6 M. Dusselier, P. Van Wouwe, F. de Clippel, J. Dijkmans, D. W. Gammon and B. F. Sels, *ChemCatChem*, 2013, **5**, 569–575.
7 W. R. Gunther, V. K. Michaelis, M. A. Caporini, R. G. Griffin and Y. Román-Leshkov, *J. Am. Chem. Soc.*, 2014, **136**, 6219–6222.
8 Y. Román-Leshkov, M. Moliner, J. A. Labinger and M. E. Davis, *Angew. Chem.*, 2010, **122**, 9138–9141.
9 H. Kim and J. Ralph, *Org. Biomol. Chem.*, 2010, **8**, 576–591.

10 Y. Pu, S. Cao and A. J. Ragauskas, *Energy Environ. Sci.*, 2011, **4**, 3154.
11 L. Botti, S. A. Kondrat, R. Navar, D. Padovan, J. S. Martinez-Espin, S. Meier and C. Hammond, *Angew. Chem.*, 2020, **132**, 20192–20198.
12 L. Botti, S. Meier and C. Hammond, *ACS Catal.*, 2021, **11**, 1296–1308.
13 D. Padovan, L. Botti and C. Hammond, *ACS Catal.*, 2018, **8**, 7131–7140.
14 M. A. Newton and W. van Beek, *Chem. Soc. Rev.*, 2010, **39**, 4845.
15 L. Dong, L. Lin, X. Han, X. Si, X. Liu, Y. Guo, F. Lu, S. Rudić, S. F. Parker, S. Yang and Y. Wang, *Chem*, 2019, **5**, 1521–1536.
16 Y. Shao, Q. Xia, L. Dong, X. Liu, X. Han, S. F. Parker, Y. Cheng, L. L. Daemen, A. J. Ramirez-Cuesta, S. Yang and Y. Wang, *Nat Commun*, 2017, **8**, 16104.
17 V. Vorotnikov, G. Mpourmpakis and D. G. Vlachos, *ACS Catal.*, 2012, **2**, 2496–2504.
18 G. Li, E. A. Pidko and E. J. M. Hensen, *Catal. Sci. Technol.*, 2014, **4**, 2241–2250.
19 G. Yang, E. A. Pidko and E. J. M. Hensen, *ChemSusChem*, 2013, **6**, 1688–1696.
20 W. Deng, P. Wang, B. Wang, Y. Wang, L. Yan, Y. Li, Q. Zhang, Z. Cao and Y. Wang, *Green Chem.*, 2018, **20**, 735–744.
21 M. S. Holm, S. Saravanamurugan and E. Taarning, *Science*, 2010, **328**, 602–605.
22 R. M. West, M. S. Holm, S. Saravanamurugan, J. Xiong, Z. Beversdorf, E. Taarning and C. H. Christensen, *J. Catal.*, 2010, **269**, 122–130.
23 L. Li, F. Shen, R. L. Smith and X. Qi, *Green Chem.*, 2017, **19**, 76–81.
24 Q. Guo, F. Fan, E. A. Pidko, W. N. P. van der Graaff, Z. Feng, C. Li and E. J. M. Hensen, *ChemSusChem*, 2013, **6**, 1352–1356.
25 I. Tosi, A. Sacchetti, J. S. Martinez-Espin, S. Meier and A. Riisager, *Top Catal*, 2019, **62**, 628–638.
26 J. Pang, M. Zheng, X. Li, L. Song, R. Sun, J. Sebastian, A. Wang, J. Wang, X. Wang and T. Zhang, *ChemistrySelect*, 2017, **2**, 309–314.
27 B. Murillo, A. Sánchez, V. Sebastián, C. Casado-Coterillo, O. de la Iglesia, M. P. López-Ram- de-Viu, C. Téllez and J. Coronas, *J. Chem. Technol. Biotechnol.*, 2014, **89**, 1344–1350.
28 J. Zhang, L. Wang, G. Wang, F. Chen, J. Zhu, C. Wang, C. Bian, S. Pan and F.-S. Xiao, *ACS Sus. Chem. Eng.*, 2017, **5**, 3123–3131.
29 X. Yang, J. Bian, J. Huang, W. Xin, T. Lu, C. Chen, Y. Su, L. Zhou, F. Wang and J. Xu, *Green Chem.*, 2017, **19**, 692–701.
30 S. Meier, M. Karlsson, P. R. Jensen, M. H. Lerche and J. Ø. Duus, *Mol. BioSys.*, 2011, **7**, 2834–2836.
31 P. R. Jensen, F. Sannelli, L. T. Stauning and S. Meier, *Chem. Comm.*, 2021, **57**, 10572–10575.
32 J. H. Ardenkjær-Larsen, B. Fridlund, A. Gram, G. Hansson, L. Hansson, M. H. Lerche, R. Servin, M. Thaning and K. Golman, *Proc. Natl. Acad. Sci. U.S.A.*, 2003, **100**, 10158–10163.
33 Y. V. Pfeifer, P. T. Haase and L. W. Kroh, *J. Agric. Food Chem.*, 2013, **61**, 3090–3096.
34 M. A. Molenda, S. Baś and J. Mlynarski, *Eur. J. Org. Chem.*, 2016, **2016**, 4394–4403.
35 J. M. De Bruijn, A. P. G. Kieboom and H. van Bekkum, *Starch/Stärke*, 1987, **39**, 23–28.
36 S. G. Elliot, I. Tosi, A. Riisager, E. Taarning and S. Meier, *Top Catal*, 2019, **62**, 590–598.
37 F. A. A. Mulder, L. Tenori and C. Luchinat, *Angew. Chem.*, 2019, **58**, 15283–15286.
38 M. Kolen, W. A. Smith and F. M. Mulder, *ACS Omega*, 2021, **6**, 5698–5704.
39 Y. Zhao, R. Liu, C. Marcus Pedersen, Z. Zhang, Z. Guo, H. Chang, Y. Wang and Y. Qiao, *J. Mol. Liq.*, 2022, **357**, 119074.
40 S. Meier, P. R. Jensen and J. Ø. Duus, *FEBS Letters*, 2011, **585**, 3133–3138.